

- Lozovik Yu E, Nishanov V N, in *Vsesoyuz. Soveshchanie po Dielektricheskoi Elektronike, Tashkent 1973. Tezisy Dokladov* (All-Union Conf. on Dielectric Electronics) (Tashkent: Fan, 1973) p. 70
75. Lozovik Yu E, Berman O L *Pis'ma Zh. Eksp. Teor. Fiz.* **64** 526 (1996) [*JETP Lett.* **64** 573 (1996)]; *Zh. Eksp. Teor. Fiz.* **111** 1879 (1997) [*JETP* **84** 1027 (1997)]
  76. Das Sarma S, Madhukar A *Phys. Rev. B* **23** 805 (1981)
  77. Wunsch B et al. *New J. Phys.* **8** 318 (2006)
  78. Nozières P, Schmitt-Rink S *J. Low Temp. Phys.* **59** 195 (1985)
  79. Kopnin N B, Sonin E B, arXiv:0803.3772
  80. Min H et al., arXiv:0802.3462
  81. Lozovik Yu E, Efimkin D K (to be published)
  82. Adam S et al. *Proc. Natl. Acad. Sci. USA* **104** 18392 (2007)
  83. Conti S, Vignale G, MacDonald A H *Phys. Rev. B* **57** R6846 (1998)
  84. Lozovik Yu E, Nikitkov M V *Zh. Eksp. Teor. Fiz.* **116** 1440 (1999) [*JETP* **89** 775 (1999)]
  85. Lozovik Yu E, Poushnov A V *Phys. Lett. A* **228** 399 (1997)
  86. Balatsky A V, Joglekar Y N, Littlewood P B *Phys. Rev. Lett.* **93** 266801 (2004)
  87. Iyengar A et al. *Phys. Rev. B* **75** 125430 (2007)
  88. Berman O L, Lozovik Yu E, Gumbs G *Phys. Rev. B* **77** 155433 (2008)
  89. Gorkov L P, Dzyaloshinskii I E *Zh. Eksp. Teor. Fiz.* **53** 717 (1967) [*Sov. Phys. JETP* **26** 449 (1968)]
  90. Lozovik Yu E, Ruvinsky A M *Phys. Lett. A* **227** 271 (1997)
  91. Lozovik Yu E, Ruvinskii A M *Zh. Eksp. Teor. Fiz.* **112** 1791 (1997) [*JETP* **85** 979 (1997)]
  92. Lozovik Yu E, Berman O L, Willander M J. *Phys.: Condens. Matter* **14** 12457 (2002)
  93. Griffin A *Excitations in a Bose-Condensed Liquid* (Cambridge: Cambridge Univ. Press, 1993)
  94. Lozovik Yu E, Yudson V I *Physica A* **93** 493 (1978)
  95. Lozovik Yu E, Berman O L, Tsvetov V G *Phys. Rev. B* **59** 5627 (1999)
  96. Lifshitz E M, Pitaevskii L P *Statisticheskaya Fizika* (Statistical Physics) (Moscow: Nauka, 1978) Vol. 2 [Translated into English (Oxford: Pergamon Press, 1980)]
  97. Berman O L, Kezerashvili R Ya, Lozovik Yu E, arXiv:0711.0976
  98. Berman O L, Kezerashvili R Ya, Lozovik Yu E *Phys. Rev. B* **78** 035135 (2008), arXiv:0801.1094
  99. Moskalenko S A et al. *Phys. Rev. B* **66** 245316 (2002)
  100. Eisenstein J P, MacDonald A H *Nature* **432** 691 (2004)
  101. Halperin B I, Lee P A, Read N *Phys. Rev. B* **47** 7312 (1993)
  102. Heinonen O (Ed.) *Composite Fermions: A Unified View of the Quantum Hall Regime* (Singapore: World Scientific, 1998)
  103. Lozovik Yu E, Prokhorenko D V (to be published)
  104. Berman O L, Lozovik Yu E, Gumbs G *Phys. Rev. B* **78** 085401 (2008)
  105. Chiu K W, Quinn J J *Phys. Rev. B* **9** 4724 (1974)
  106. Eguiluz A et al. *Phys. Rev. B* **11** 4989 (1975)
  107. Das Sarma S, Quinn J J *Phys. Rev. B* **25** 7603 (1982)
  108. Zhang Y et al. *Phys. Rev. Lett.* **96** 136806 (2006)
  109. Jiang Z et al. *Phys. Rev. Lett.* **99** 106802 (2007)
  110. Abanin D A et al. *Phys. Rev. Lett.* **98** 196806 (2007)
  111. Shibata N, Nomura K, arXiv:0803.2418
  112. Cortijo A, Vozmediano M A H, arXiv:0709.2698
  113. Katsnelson M I *Eur. Phys. J. B* **51** 157 (2006); Tworzydło J et al. *Phys. Rev. Lett.* **96** 246802 (2006)
  114. Huard B et al. *Phys. Rev. Lett.* **98** 236803 (2007)
  115. Nair R R et al. *Science* **320** 1308 (2008); arXiv:0803.3718
  116. Dobryakov A L et al. *Zh. Eksp. Teor. Fiz.* **119** 309 (2001) [*JETP* **92** 267 (2001)]
  117. Das Sarma S, Hwang E H, Tse W-K *Phys. Rev. B* **75** 121406(R) (2007)
  118. Le Doussal P, Radzihovsky L *Phys. Rev. Lett.* **69** 1209 (1992)
  119. Fasolino A, Los J H, Katsnelson M I *Nature Mater.* **6** 858 (2007); Abedpour N et al. *Phys. Rev. B* **76** 195407 (2007)
  120. Chen Z et al. *Physica E* **40** 228 (2007); Lemme M C et al. *IEEE Electron Device Lett.* **28** 282 (2007)
  121. Echtermeyer T J et al., arXiv:0712.2026
  122. Zhou S Y et al. *Nature Mater.* **6** 770 (2007)
  123. Stampfer C et al. *Appl. Phys. Lett.* **92** 012102 (2008); Ponomarenko L A et al. *Science* **320** 356 (2008)
  124. Žutić I, Fabian J, Das Sarma S *Rev. Mod. Phys.* **76** 323 (2004)
  125. Hill E W et al. *IEEE Trans. Magn.* **42** 2694 (2006); Ohishi M et al. *Jpn. J. Appl. Phys.* **46** L605 (2007); Cho S, Chen Y-F, Fuhrer M S *Appl. Phys. Lett.* **91** 123105 (2007)
  126. Xiao D, Yao W, Niu Q *Phys. Rev. Lett.* **99** 236809 (2007); Yao W, Xiao D, Niu Q *Phys. Rev. B* **77** 235406 (2008); Rycerz A *Phys. Status Solidi A* **205** 1281 (2008)
  127. Boukhvalov D W, Katsnelson M I, Lichtenstein A I *Phys. Rev. B* **77** 035427 (2008)
  128. Stankovich S et al. *Nature* **442** 282 (2006)
  129. Schedin F et al. *Nature Mater.* **6** 652 (2007)
  130. Blake P et al., arXiv:0803.3031
  131. Bunch J S et al. *Science* **315** 490 (2007)
  132. Lusk M T, Carr L D *Phys. Rev. Lett.* **100** 175503 (2008)
  133. Sevincli H, Topsakal M, Ciraci S, arXiv:0711.2414
  134. Park C-H et al. *Nature Phys.* **4** 213 (2008)

PACS numbers: 72.80.Rj, **73.43.-f**, 81.05.Uw  
DOI: 10.1070/PU2008v051n07ABEH006575

## Electron transport in graphene

S V Morozov, K S Novoselov, A K Geim

### 1. Two-dimensional crystals

Carbon is an amazing chemical element that produces the most diverse structures. In addition to graphite and diamond, known since time immemorial, the attention of the scientific community is now focused on the recently discovered fullerenes [1–3] and nanotubes [4]. Unfortunately, experimenters could only work with three-dimensional (graphite, diamond), one-dimensional (nanotubes), and zero-dimensional (fullerenes) forms of carbon because all attempts to prepare specimens of two-dimensional carbon were unsuccessful until recently.

This mysterious two-dimensional form (planar hexagonal packing of carbon atoms) was called graphene and surprisingly happened to become perhaps the most studied among all carbon allotropes: indeed, graphene is the starting point for all calculations related to graphite, fullerenes, and nanotubes. At the same time, the numerous attempts to synthesize such two-dimensional crystals all failed, with only nanometer-scale crystallites obtained [5]. This was not surprising, however, in view of the prevailing opinion that truly two-dimensional crystals cannot exist [6–10] (in contrast to familiar quasi-two-dimensional systems). Indeed, graphene seeds should have a very high perimeter-to-surface-area ratio in the course of synthesis, which should facilitate transformation to other carbon allotropes.

This continued until 2004, when a group of researchers in Manchester and Chernogolovka employed a surprisingly simple and even naive approach to prepare graphene (Fig. 1), which made graphene one of the hottest topics in modern solid state physics [11, 12]. A separate plane (of monatomic thickness) was segregated from a three-dimensional graphite crystal using so-called micromechanical cleavage (graphite is a spectacularly lamellar material and can be treated as a stack of two-dimensional graphene crystals only weakly bonded to one another). Furthermore, two-dimensional crystals of other materials were also obtained by this technique [12], e.g., boron nitride, some dichalcogenides, and a high-temperature superconductor Bi–Sr–Ca–Cu–O. In fact, a new class of materials was born—two-dimensional crystals, stable in the free state.

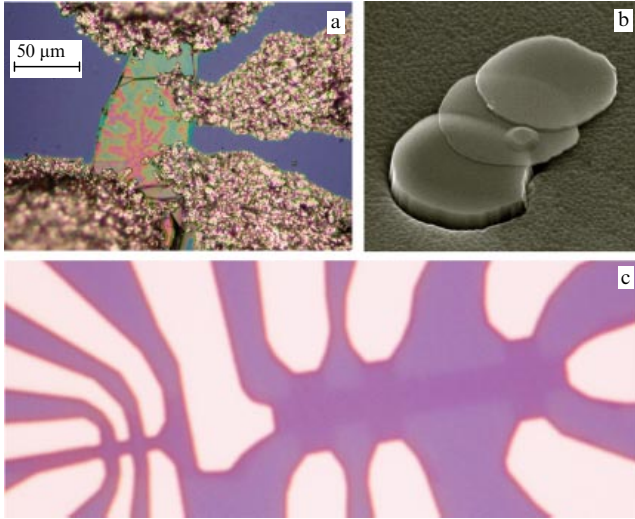


**Figure 1.** (a) A photograph of the first Hall transistor made on thin graphite film. Electron microscope image of cleaved graphite microdisks (b) and and Hall transistor (c) (channel width: 1  $\mu\text{m}$ ).

Remarkably, this relatively simple method led to preparing sufficiently large crystallites (up to 100  $\mu\text{m}$ ) and immediately stimulated great experimental activity [13]. Moreover, the quality of the obtained material proved to be so high that it was possible to implement ballistic transport [11, 14] and to observe the quantum Hall effect [15, 16]. The properties of this new material allow characterizing it as a very promising candidate for future microelectronic devices, such as the ballistic field transistor. However, even though the technique that we proposed does provide the best available graphene in laboratory conditions, industrial application demands more productive technologies. Today, the technology of cleaving using graphite intercalation [17–21] and epitaxy of graphene by sublimation of silicon off the surface of a SiC substrate [22, 23] are more successful.

## 2. Linear dispersion

By its electron properties, graphene is a two-dimensional semiconductor with a zero-width band gap (Fig. 2). Quasiparticles in graphene are formally described by the Dirac-type Hamiltonian  $H = -i\hbar v_F \sigma \nabla$ , where  $v_F \approx 10^6 \text{ m s}^{-1}$  is the Fermi velocity and  $\sigma = (\sigma_x, \sigma_y)$  are the Pauli matrices [24–27]. This description, which is theoretically correct if we ignore multiparticle effects, was confirmed in experimental measurements [15] of the cyclotron mass of charge carriers in graphene as a function of their energy (Fig. 3). These measurements confirmed that quasiparticles in graphene obey a linear dispersion law. The observation of the relativistic analog of the integral quantum Hall effect is perhaps the most impressive manifestation of this; we discuss it in Section 4.

The fact that charge carriers in graphene are described not by the Schrödinger equation, which is more standard in solid state physics, but by the Dirac equation results from the symmetry of the graphene crystal lattice, which consists of two equivalent carbon sublattices A and B (see Fig. 2). Electron subbands formed by a symmetric and an asymmetric combination of wave functions on these two sublattices overlap at the edge of the Brillouin zone, which

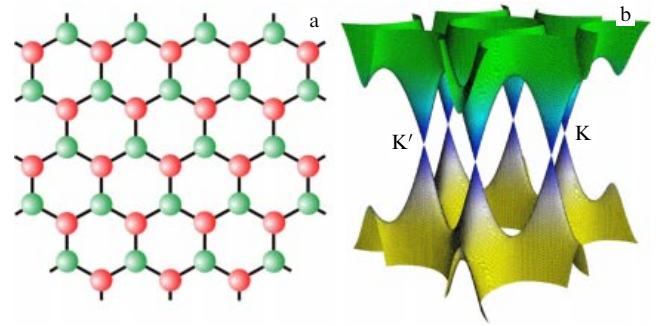


**Figure 2.** (a) The crystal structure of graphene. Two sublattices are marked by different colors. (b) Graphene band structure: the conduction band and valence band touch at the points K and K'.

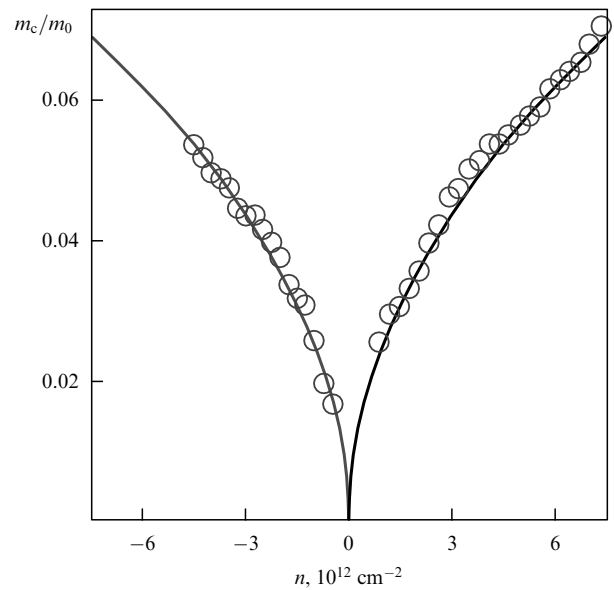


**Figure 3.** Experimental curves of the cyclotron mass of electrons and holes as functions of the charge carrier concentration in graphene. The square root dependence is an indication of a linear dispersion law.

results in a cone-shaped energy spectrum close to the ‘Dirac’ points K and K'. As a consequence, quasiparticles in graphene, like massless relativistic particles, have the linear dispersion law  $E = \hbar k v_F$ , where the Fermi velocity  $v_F \approx c/300$  plays the role of the speed of light. In view of the linearity of the spectrum, we can expect the behavior of quasiparticles in graphene to be principally different from the behavior of quasiparticles in ordinary metals and semiconductors, where they have parabolic dispersion and behave like free electrons.

The linear dispersion law is the most important but definitely not the only specific feature of quantum transport that follows from the Dirac equation. Current-carrying states at positive energies (above the Dirac point) are similar to electrons and are negatively charged. If the valence band is not fully occupied at negative energies, then quasiparticles behave as positively charged particles (holes) and can be treated as a solid-state analog of positrons. We note, however, that in solid state physics, electrons and holes are typically described by independent Schrödinger equations, each with its own effective mass (in accordance with the Seitz sum rule). In contrast to this, electrons and holes in graphene are interrelated and display properties of charge-conjugation

symmetry. In graphene, this follows from the symmetry of its crystal lattice and from the fact that quasiparticles in graphene are described by a two-component wave function based on sublattices A and B. The two-component description of graphene is analogous to the description in quantum electrodynamics (QED) involving spinor wave functions, but in the case of graphene, the ‘spin’ index stems from its belonging to different sublattices and not to the ‘real’ spin of ordinary electrons, and is usually referred to as pseudospin  $\sigma$ .

Other similarities with QED exist. The conical shape of the dispersion law in graphene is a result of overlapping of subbands due to superlattices A and B. Therefore, electrons at an energy  $E$  moving in the positive direction belong to the same branch of the spectrum as holes at the energy  $-E$  moving in the opposite direction. This means that electrons and holes sitting on the same branch of the spectrum have the same pseudospin, which is parallel to the quasimomentum for electrons and antiparallel to it for holes. This allows the introduction of chirality [27], which is the projection of the pseudospin onto the direction of motion and has positive sign for electrons and negative sign for holes.

The same effects can be described semiclassically in terms of the so-called Berry phase. Because the wave functions of electrons are two-component spinors, they switch sign when an electron follows a closed path. Wave functions thus gain an additional Berry phase equal to  $\pi$ .

### 3. The effect of an electric field

Most experimental groups have so far used specimens prepared by the original micromechanical cleavage technique [11, 12], which allows producing high-quality two-dimensional crystals up to  $1000 \mu\text{m}^2$  in area; this is sufficient for most experiments. The key to the success of this method lies in graphene becoming visible in an optical microscope when it is placed on a plate of oxidized silicon with a precisely chosen thickness of the  $\text{SiO}_2$  layer: this creates a contrast, albeit a weak one, with the clean substrate [28]. Were it not for this rather simple but efficient method of scanning the substrate in search of individual graphene crystals, graphene would most probably still remain undiscovered. Even if we forget about earlier theoretical arguments that put the existence of two-dimensional crystals in doubt in principle, the current research methods of studying one-atom-thick and small objects (e.g., scanning atomic force microscopy) have unacceptably low productivity for locating scarce and isolated graphene crystals. Scanning electron microscopy has a higher productivity but can hardly distinguish between crystals of different thicknesses. We note, however, that Raman spectroscopy does distinguish between graphene and multilayer crystals and can be used to identify it [29, 30], even though it requires preselection by optical means.

The  $\text{SiO}_2$  substrate is also an insulation layer. Consequently, doped silicon acts as a gate and helps control the concentration of charge carriers in graphene. The charge carrier type can thus be changed from electron to hole (Fig. 4). Charge carrier concentrations up to  $10^{13} \text{cm}^{-2}$  can be achieved in electric fields at which electric breakdown of the insulator sets in. High carrier mobility (up to  $20,000 \text{cm}^2 \text{B}^{-1} \text{s}^{-1}$ ), depending only weakly on temperature, is still sustained in the entire range of concentration [11]. As a result, ballistic transport on a submicron scale is realized even at room temperature. Charge carrier mobility, which is limited in current specimens of graphene by impurities or

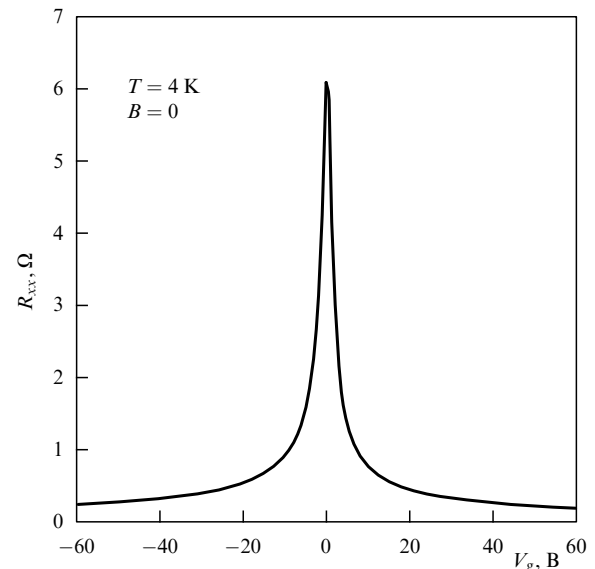


**Figure 4.** The ambipolar effect of an electric field in graphene. Positive (negative) gate voltage induces electrons (holes) with the concentration  $n = \alpha V_g$  where  $\alpha \approx 7.2 \times 10^{10} \text{cm}^{-2} \text{B}^{-1}$  for the  $\text{SiO}_2$  insulating gate layer thickness 300 nm.

the nanorippling of crystals, can potentially be improved enormously: by our experimental evaluations, it is bounded above by  $200,000 \text{cm}^2 \text{B}^{-1} \text{s}^{-1}$  due to phonon scattering [31].

Another unusual feature of graphene is that its conductivity remains finite even as the charge carrier concentration  $n$  tends to zero; moreover, its value approaches the conductivity quantum  $4e^2/h$  [15]. It must be emphasized that in contrast to other familiar quantum transport effects, it is the conductivity which is quantized, not conductance. The minimum of quantum conductivity for Dirac fermions was predicted in theoretical papers [32–38]. In some of them, the key moment is the density of states tending to zero in the vicinity of the Dirac point on the linear two-dimensional spectrum. At the same time, two-monolayer graphene with the parabolic dispersion law of quasiparticles also displays conductivity that has a minimum of the order of  $4e^2/h$ , which specifically points to the importance of chirality and not of the linear spectrum [39]. Furthermore, most theories predict a minimum conductivity lower by a factor of  $\pi$  than the experimentally observed value. This contradiction is known as ‘the mystery of the missing pi’ and it is still unclear whether this is a consequence of theoretical approximations or stems from the limited parameters of experimental specimens. Thus, experiments show that at low concentrations ( $< 10^{11} \text{cm}^{-2}$ ), charge carriers in graphene break into a network of ‘puddles’ of electrons and holes. This microscopic inhomogeneity must definitely be present near the Dirac point but has not yet been taken into account in theoretical papers. Also, macroscopic inhomogeneities may play an important role in experiments (on a scale exceeding the free path length). Available experimental experience indicates that in more homogeneous specimens, e.g., for smaller sizes or after soft annealing, the spread of the minimum conductivity  $4e^2/h$  is smaller.

### 4. The quantum Hall effect in graphene

The main experimental effort following the discovery of graphene was aimed at studying the electric properties of

graphene that would confirm that the quasiparticles in it are indeed described by QED. Two new ('chiral') effects of a quantum Hall effect (QHE) type were among the most spectacular manifestations of this.

Figure 5 illustrates the QHE in graphene. The QHE in monolayer graphene is observed as a series of equidistant steps of the Hall conductivity  $\sigma_{xy}$ , which passes through zero at the point of electric neutrality (the Dirac point), where the hole conductivity changes to the electron type. The sequence of plateaus has the expected step height but is shifted by  $1/2$  compared with the 'standard' curve, such that the Hall conductivity takes the form

$$\sigma_{xy} = 4 \frac{e^2}{h} \left( N + \frac{1}{2} \right),$$

where  $N$  is an integer and the factor 4 reflects the double spin and valley degeneracy. In monolayer graphene, we thus have the 'half-integral' QHE. This unusual behavior is well understood now: it occurs because of the specifics of quantization of Dirac fermions in graphene with linear dispersion in the magnetic field  $B$ , and is described by the expression  $E_N = \pm v_F \sqrt{2e\hbar BN}$ , where  $+$  and  $-$  respectively refer to electrons and holes [26, 27, 40–42]. The essential observation is that there is the zeroth Landau level at  $E = 0$  (Fig. 6), which simultaneously belongs to electrons and holes; this explains the unusual quantization of the Hall conductivity [39, 41, 42].

An alternative interpretation of the reasons for the half-integer QHE starts with the fact that the superposition of pseudospin and orbital motion results in giving electrons an additional Berry phase of  $\pi$ ; it is accumulated along the cyclotron trajectory. The additional phase results in a half-period phase shift of quantum oscillations and a shift of Hall plateaus by  $1/2$  after the transition to the quantum Hall effect mode [15, 16].

The linear spectrum in graphene and the high value of the Fermi velocity result in enormous orbital splitting. The distance between the  $N = 0$  and  $N = 1$  Landau levels equals  $\Delta E \approx 400 \text{ [K]} \sqrt{B}$ , where  $B$  is the magnetic field in teslas. This means that the splitting of the first levels at  $B = 30 \text{ T}$  is approximately 2200 K, which exceeds room temperature by

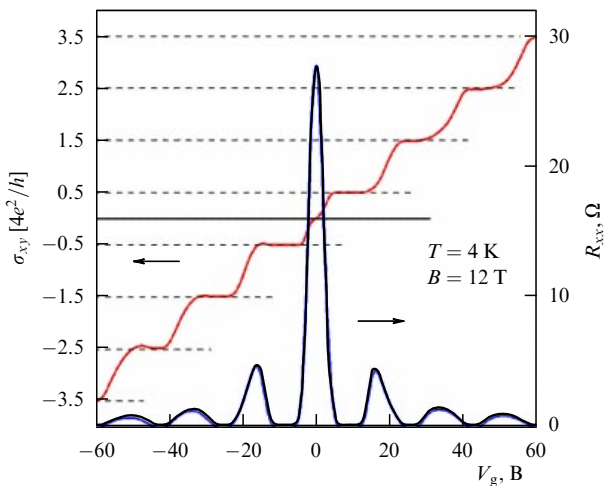


**Figure 5.** Longitudinal magnetoresistance and Hall conductivity in graphene as functions of gate voltage. Half-integral quantization confirms that quasiparticles in graphene are massless Dirac fermions.

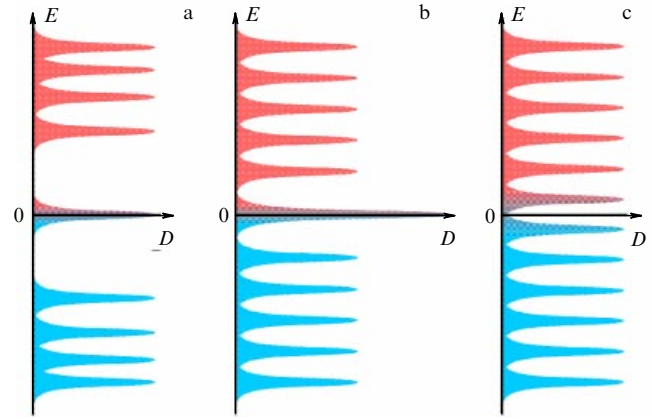


**Figure 6.** Landau levels for massless Dirac electrons in monolayer graphene (a), for massive chiral electrons in two-monolayer graphene (b), and for Schrödinger electrons with two parabolic zones tangent at the point of zero energy (c).

almost an order of magnitude. Moreover, very weak dependence of the carrier mobility on temperature in graphene creates conditions for the inequality  $\mu B \gg 1$  to hold already for  $B$  of only several teslas. As a result, it is possible to observe the quantum Hall effect even at room temperature [43]; this may prove important for metrology.

In quantum electrodynamics, chirality is directly related to the relativistic nature of particles and correspondingly to the linear dispersion law for massless particles. The discovery of graphene gives us a possibility of studying another principally new type of particle: chiral quasiparticles with a parabolic (nonrelativistic) dispersion law that we find in two-monolayer graphene [39]. According to theoretical calculations [39, 44], two-monolayer graphene is a semiconductor with a zero band gap but, in contrast to multilayered graphene, its valence band and conduction band are parabolic and touch at the points  $K$  and  $K'$  of the Brillouin zone. At the same time, quasiparticles in two-monolayer graphene, just as in monolayer graphene, have chirality but also gain the Berry phase  $2\pi$  (and not  $\pi$ ). The exact quantum mechanical solution [39, 44] for quasiparticles of this type gives the following values of energy for Landau levels:  $E_N \propto \sqrt{N(N-1)}$ . Therefore, at zero energy, we again find a Landau level, but the multiplicity of its degeneracy is twice that of the other levels. Landau levels beyond the ultraquantum limit ( $N > 1$ ) are practically equidistant in energy, just as they are in the case of constant-mass electrons. As a result, the QHE of two-monolayer graphene differs from the QHE both in graphene monolayers and in the two-dimensional electron gas of ordinary semiconductors.

As noted in Section 2, the Dirac description of quasiparticles in graphene stems directly from two-component wave functions of quasiparticles reflecting the symmetry of the crystal lattice of multilayer graphene, and from the presence of two superlattices A and B. The situation in two-monolayer graphene is to a large extent similar but the superlattices are now separated into different monolayers. In that case, we are offered a unique chance of influencing these superlattices differently and separately. Thus, an external perpendicular electric field removes degeneracy at the  $K$  points and creates a band gap [44–46]. This effect manifests itself in the QHE regime as the zero plateau emerging in the Hall conductivity



[46]. It is important that the gap width in achievable electric fields may vary from 0 to 0.3 eV, which may be very promising for applications.

## 5. Conclusion

Graphene became the first and is so far the most vivid representative of a new class of materials—two-dimensional crystals. In fact, graphene opened a new scientific paradigm—‘relativistic’ solid state physics in which quantum relativistic phenomena, some of which cannot be implemented even in high-energy physics, can be studied under ordinary laboratory conditions. What makes the electron properties of graphene unique is the fact that charge carriers in it resemble massless relativistic fermions and are described by the relativistic Dirac equation, not the Schrödinger equation. This is the first time that we can study all the subtleties and the rich variety of quantum electrodynamics in solid-state experiments.

Graphene immediately emerged as a realistic candidate for the role of one of the main materials for microelectronics in the post-silicon era. Suffice it to mention the first prototypes of future graphene-based devices. These are room-temperature field transistors with ballistic transport, extremely sensitive gas sensors [47], one-electron graphene transistors [48], liquid-crystal displays and solar batteries (in which graphene is used as a transparent conducting electrode) [49], spin transistors [50], and many others. Graphene’s history is short but is undoubtedly at the very start of its climb.

**Acknowledgments.** S V M is grateful for the financial support to the RFBR (grant 08-02-01067) and RAS programs.

## References

1. Curl R F *Rev. Mod. Phys.* **69** 691 (1997); *Usp. Fiz. Nauk* **168** 331 (1998)
2. Kroto H *Rev. Mod. Phys.* **69** 703 (1997); *Usp. Fiz. Nauk* **168** 343 (1998)
3. Smalley R E *Rev. Mod. Phys.* **69** 723 (1997); *Usp. Fiz. Nauk* **168** 323 (1998)
4. Iijima S *Nature* **354** 56 (1991)
5. Oshima C, Nagashima A *J. Phys.: Condens. Matter* **9** 1 (1997)
6. Peierls R E *Helv. Phys. Acta* **7** 81 (1934)
7. Peierls R E *Ann. Inst. Henri Poincaré* **5** 177 (1935)
8. Landau L D *Phys. Z. Sowjetunion* **11** 26 (1937)
9. Landau L D, Lifshitz E M *Statisticheskaya Fizika* (Statistical Physics) Pt. 1 (Moscow: Nauka, 1976) [Translated into English (Oxford: Pergamon Press, 1980)]
10. Mermin N D *Phys. Rev.* **176** 250 (1968)
11. Novoselov K S et al. *Science* **306** 666 (2004)
12. Novoselov K S et al. *Proc. Natl. Acad. Sci. USA* **102** 10451 (2005)
13. Geim A K, Novoselov K S *Nature Mater.* **6** 183 (2007)
14. Morozov S V et al. *Phys. Rev. B* **72** 201401(R) (2005)
15. Novoselov K S et al. *Nature* **438** 197 (2005)
16. Zhang Y et al. *Nature* **438** 201 (2005)
17. Dresselhaus M S, Dresselhaus G *Adv. Phys.* **51** 1 (2002)
18. Shioyama H *J. Mater. Sci. Lett.* **20** 499 (2001)
19. Viculis L M, Mack J J, Kaner R B *Science* **299** 1361 (2003)
20. Horiuchi S et al. *Appl. Phys. Lett.* **84** 2403 (2004)
21. Stankovich S et al. *J. Mater. Chem.* **16** 155 (2006)
22. Van Bommel A J, Crombeen J E, Van Tooren A *Surf. Sci.* **48** 463 (1975)
23. Berger C et al. *J. Phys. Chem. B* **108** 19912 (2004)
24. Wallace P R *Phys. Rev.* **71** 622 (1947)
25. Slonczewski J C, Weiss P R *Phys. Rev.* **109** 272 (1958)
26. McClure J W *Phys. Rev.* **104** 666 (1956)
27. Haldane F D M *Phys. Rev. Lett.* **61** 2015 (1988)
28. Blake P et al. *Appl. Phys. Lett.* **91** 063124 (2007)
29. Ferrari A C et al. *Phys. Rev. Lett.* **97** 187401 (2006)
30. Graf D et al. *Nano Lett.* **7** 238 (2007)
31. Morozov S V et al. *Phys. Rev. Lett.* **100** 016602 (2008)
32. Katsnelson M I *Eur. Phys. J. B* **51** 157 (2006)
33. Tworzydło J et al. *Phys. Rev. Lett.* **96** 246802 (2006)
34. Fradkin E *Phys. Rev. B* **33** 3263 (1986)
35. Lee P A *Phys. Rev. Lett.* **71** 1887 (1993)
36. Ludwig A W W et al. *Phys. Rev. B* **50** 7526 (1994)
37. Ziegler K *Phys. Rev. Lett.* **80** 3113 (1998)
38. Nomura K, MacDonald A H *Phys. Rev. Lett.* **96** 256602 (2006)
39. Novoselov K S et al. *Nature Phys.* **2** 177 (2006)
40. Zheng Y, Ando T *Phys. Rev. B* **65** 245420 (2002)
41. Gusynin V P, Sharapov S G *Phys. Rev. Lett.* **95** 146801 (2005)
42. Peres N M R, Guinea F, Castro Neto A H *Phys. Rev. B* **73** 125411 (2006)
43. Novoselov K S et al. *Science* **315** 1379 (2007)
44. McCann E, Fal’ko V I *Phys. Rev. Lett.* **96** 086805 (2006)
45. Ohta T et al. *Science* **313** 951 (2006)
46. Castro E V et al. *Phys. Rev. Lett.* **99** 216802 (2007)
47. Schedin F et al. *Nature Mater.* **6** 652 (2007)
48. Ponomarenko L A et al. *Science* **320** 356 (2008)
49. Blake P et al. *Nano Lett.* (2008), to be published
50. Hill E W et al. *IEEE Trans Magn.* **42** 2694 (2006)